chemistry

MDPI

Communication

Mechanochemistry through Extrusion: Opportunities for Nanomaterials Design and Catalysis in the Continuous Mode

Oscar Trentin [1], Daniele Polidoro [1], Alvise Perosa [1], Enrique Rodríguez-Castellon [2], Daily Rodríguez-Padrón [1,*] and Maurizio Selva [1,*]

[1] Department of Molecular Science and Nanosystems, Ca' Foscari University of Venice, Via Torino 155, 30175 Venezia, Italy; 876032@stud.unive.it (O.T.); daniele.polidoro@unive.it (D.P.); alvise@unive.it (A.P.)
[2] Department of Inorganic Chemistry, Facultad de Ciencias, Universidad de Málaga, Campus de Teatinos s/n, 29071 Málaga, Spain; castellon@uma.es
* Correspondence: daily.rodriguez@unive.it (D.R.-P.); selva@unive.it (M.S.)

Abstract: The potentialities of mechanochemistry trough extrusion have been investigated for the design of nanosized catalysts and their use in C-C bond-forming reactions. The mechanochemical approach proved successful for the synthesis of supported palladium nanoparticles with mean diameter within 6–10 nm, achieved by the reduction of Pd(II) acetate with ethylene glycol, in the absence of any solvent. A mesoporous N-doped carbon derived from chitin as a renewable biopolymer, was used as a support. Thereafter, the resulting nanomaterials were tested as catalysts to implement a second extrusion based-protocol for the Suzuki-Miyaura cross-coupling reaction of iodobenzene and phenylboronic acid. The conversion and the selectivity of the reaction were 81% and >99%, respectively, with a productivity of the desired derivative, biphenyl, of 41 mmol g_{cat}^{-1} h^{-1}.

Keywords: mechanochemistry; extrusion; catalytic nanomaterials; Suzuki-Miyaura cross-coupling reaction

Citation: Trentin, O.; Polidoro, D.; Perosa, A.; Rodríguez-Castellon, E.; Rodríguez-Padrón, D.; Selva, M. Mechanochemistry through Extrusion: Opportunities for Nanomaterials Design and Catalysis in the Continuous Mode. *Chemistry* **2023**, *5*, 1760–1769. https://doi.org/10.3390/chemistry5030120

Academic Editor: Mark Mascal

Received: 29 June 2023
Revised: 2 August 2023
Accepted: 4 August 2023
Published: 8 August 2023

1. Introduction

In recent years, mechanochemistry has emerged as a promising avenue for the synthesis and design of nanomaterials with an environmentally friendly perspective [1]. Due to their simplicity and cost-efficiency, mechanochemical strategies have been implemented to prepare a variety of nanomaterials including supported metal nanoparticles or biomass-templated metal oxides to perovskites and bioconjugates [2–11]. Thrilling opportunities for mechanochemistry are also found in the field of organic synthesis, to obtain peptides, DNA fragments or even active pharmaceutical ingredients [12–18]. This scenario testifies to the tremendous versatility and potential of this branch of chemistry, which aims at improving the sustainability of chemical processes by exploiting the mechanical energy typically generated from grinding, milling, and extrusion, to promote reactions. The most common techniques make use of planetary ball mills, mixer mills, drum mills, or cryomills that are limited to batch conditions. Although these procedures are efficient in conducting mechanochemically assisted transformations, ref. [1] and in some cases, accurate on the temperature control, ref. [19–21], the combined contributions of mechanical and thermal energy inputs are often hardly differentiated.

Far more promising in this respect are continuous flow (CF) mechanochemical reactors which not only allow a better control of the reaction parameters compared to conventional batch systems but are excellent in designing scalable applications. Extrusion is particularly suitable to this scope since, in a typical process, solid reactants, fed and confined under high pressure, are constantly subjected to shear forces originated by one or more screws, which induce the deformation, comminution, and activation of surface species throughout the passage in the CF-reactor [22]. Under such conditions, the mixing of different components, the temperature of the mixture, the solid-state diffusion, and, finally, the physical and

chemical changes in reagents, are tuned by the screw speed and the residence time, so that both the product's distribution and the corresponding yields can be optimized [23,24].

Extrusion also provides a platform for the synthesis of heterogeneous catalysts with tailored functionalities, where different precursors or additives are incorporated into each other during the (extrusion) process, to achieve nanocomposites and hybrid materials with improved mechanical strength and enhanced surface reactivity. Excellent examples have been described in the preparation of the supported metal nanoparticles used to catalyzed C-C bond forming and cross-coupling reactions via extrusion [25]. Among the most renowned strategies for C-C bond formation, the Suzuki-Miyaura cross-coupling reaction has gained significant attention in recent years for its environmentally friendly nature. The sustainability of the reaction can indeed be optimized through several key considerations. One approach is based on the use of green and renewable solvents such as water, ethanol, and bio-based derivatives or, alternatively, on solvent-less procedures. The latter, for instance, can be achieved through mechanochemical methods such as extrusion. Additionally, the design of recyclable and reusable heterogeneous catalysts can greatly reduce the carbon footprint of the reaction and improve the cost efficiency. Promising results have already been reported with cheap and non-toxic catalysts based on non-endangered metals such as nickel and copper [26–30]. However, Pd-based catalysts continue to be recognized as some of the most popular systems for the Suzuki-Miyaura cross-coupling [31–34]. Herein, a mechanochemical approach through extrusion was designed through the preparation of such catalytic materials by using palladium acetate as a metal precursor, ethylene glycol as a green reducing agent, and chitin for the synthesis of the catalyst support [35]. Chitin was selected not only for its natural abundance, but also for its high content of nitrogen, which made it an excellent candidate to produce N-doped carbons [36–38]. Notably, such (N-doped) carbons can serve as catalysts by themselves, for base-catalyzed reactions and/or facilitate the incorporation and dispersion of metal entities, mostly thanks to the presence of pyridinic surface groups.

2. Materials and Methods

Materials and equipment. Iodobenzene, phenylboronic acid, K_2CO_3, Na_2CO_3, ethylene glycol, ethanol, 2-propanol, chitin, and $Pd(Ac)_2$ were commercially available compounds sourced from Sigma-Aldrich. If not otherwise specified, reagents and solvents were employed without further purification. Gas Chromatography-Mass Spectrometry (GC-MS) (Electron Ionization (EI), 70 eV) analyses were performed on a HP5-MS capillary column (L = 30 m, Ø = 0.32 mm, film = 0.25 mm). GC (flame ionization detector; FID) analyses were performed with an Elite-624 capillary column (L = 30 m, Ø = 0.32 mm, film = 1.8 mm). All reactions were performed in duplicate to verify reproducibility.

Synthesis of supported palladium nanoparticles on chitin-derived N-doped carbonaceous materials. The materials were prepared following a mechanochemical trough extrusion approach employing chitin (5 g) with a $Pd(Ac)_2$ (0.5 mmol) and ethylene glycol (15 mL). The mixture was extruded at 200 °C and at 50 rpm. The resulting material was oven dried at 100 °C under vacuum overnight and further employed in the catalytic tests. In addition, a thermal treatment at 500 °C (heating rate was 5 °C/min) for 1 h under N_2 flow (10 mL min^{-1}) for 1 h was carried out and the resulting material was also tested for comparison. The syntheses were performed, also adding Na_2CO_3 (0.5 mmol) under the conditions previously described.

Material Characterization. The crystalline structure of the samples was investigated by X-ray Diffraction (XRD) in the D8 Advance diffractometer of Bruker® AXS (Berlin, Germany), using the X-ray source of the Cu Kα radiation, coupled to a Lynxeye detector, and monitoring the 2θ within 8–80° at a rate of 0.08° min^{-1}. The textural properties, i.e., surface area, the volume of the pore, and pore size were determined from N_2 physisorption at 77 K, performed in ASAP 2000 equipment from Micromeritics® (Norcross, GA, USA). The samples were outgassed at 120 °C for 2 h. Then, adsorption–desorption isotherms were recorded at −196 °C. The specific surface areas were calculated by the BET method; the

pore volumes were calculated from adsorption isotherms and the pore size distributions were estimated using the Barrett, Joyner, and Halenda (BJH) algorithm available as a built-in software from Micromeritics. ICP-OES analysis was carried out in the Avio 550 Max ICP-OES Optical Emission Spectrometer.

Typical CF-Mechanochemical Suzuki-Miyaura cross-coupling reaction. The performance of the catalysts was evaluated under mechanochemical continuous flow conditions in the ZE 12 HMI extruder from Three Tec. In a typical reaction, iodobenzene (2 mmol); $PhB(OH)_2$ (3 mmol); K_2CO_3 (4 mmol), and the selected catalysts (40 mg) were extruded at 80 °C, 50 rpm, with a residence time of 1 h. Conversion and selectivity were determined by GC-FID and the product structures were assigned by GC-MS. Characterization data are available in the SI Section, Figures S1–S4.

3. Results and Discussion

The preparation of the catalysts through extrusion was carried out according to the procedure schematized in Figure 1. The experimental parameters were chosen based on the previous experience of our research group on the mechanochemical synthesis of nanomaterials [1,39,40]. A suspension of palladium acetate (0.50 mmol, 112 mg), ethylene glycol (15 mL, 0.26 mol), and chitin (5 g) was fed to a mini-extruder (ZE 12 HMI extruder from Three Tec., Seon, Switzerland) heated to 200 °C, whose conveying screws were set to 50 rpm at a torque of 2 Nm. At the end of the extrusion segment, a material in the form of small cylindrical pieces (ca 1 mm diameter) was recovered and used either as such or after a thermal treatment at 500 °C under N_2 atmosphere, to catalyze C-C bond forming reactions as Suzuki-Miyaura cross-couplings (see below). A variation of this procedure was designed by adding Na_2CO_3 (53 mg, 0.5 mmol) to the reacting mixture in order to enhance the basic properties of the sample. Overall, the four prepared materials were labelled as: Pd-chitin and Pd-chitin-500, in order to describe the catalysts achieved without and with calcination in the absence of a base, respectively, and Pd-chitin-Na_2CO_3 and Pd-chitin-Na_2CO_3-500, in order to describe the catalysts obtained without and with calcination in the presence of Na_2CO_3, respectively.

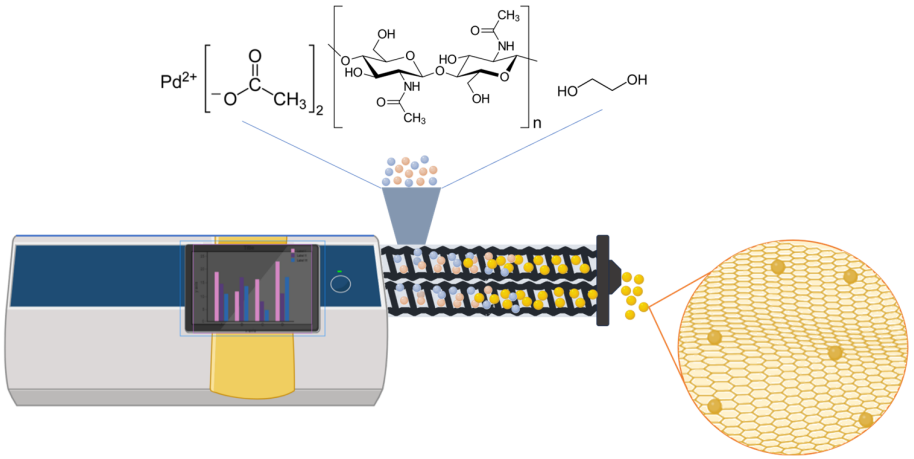

Figure 1. Schematic representation of the mechanochemically assisted synthesis of catalytic materials.

The crystal structure and arrangement of the samples were evaluated by XRD analysis. Figure 2A depicts the XRD patterns of the samples before the thermal treatment, while Figure 2B shows the results for the calcined samples. The Pd-chitin and Pd-chitin-Na_2CO_3 materials displayed the typical diffraction peaks of chitin at ca. 10, 20, 21, 23, and 26°, related to the (020), (110), (120), (101), and (130) crystallographic planes, respectively [41,42]. The overlapping of a wide peak observed in the region between 20 and 30° was most likely due to the presence of amorphous carbon formed during the mechanochemical synthesis of 200 °C. In addition, the presence of a signal at 39° indicated the (successful) reduction of palladium (II) and the formation Pd(0) nanoparticles. In Figure 2B, instead, the complete

disappearance of the typical chitin peaks, and the simultaneous presence of a wide signal at ca. 24°, were consistent with the decomposition of chitin into amorphous carbon due to the thermal treatment at 500 °C. The sharp and well-defined crystallographic peaks at 39, 47, and 68° were attributed to the (111), (200), and (220) crystallographic planes of Pd(0), respectively [43–45].

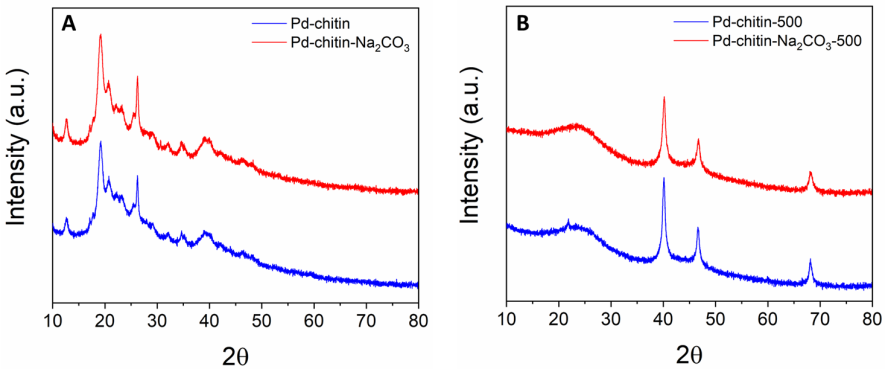

Figure 2. XRD pattern of the catalytic materials (**A**): before and (**B**): after calcination.

For comparison, the SI section reports the XRD data for commercial chitin, while the XRD diffraction patterns of palladium acetate and Na_2CO_3 are available in the literature [46,47].

The two calcined samples with and without the base, which presented consistent and clearer Pd diffraction signals, were further characterized. The results are reported in Table 1. From the XRD diffraction patterns, metal particle sizes of (6.7 ± 0.5) and (9.7 ± 0.5) nm for Pd-chitin-500 and Pd-chitin-Na_2CO_3-500, respectively, were calculated using the Scherrer equation [48,49]. The palladium loading, determined by ICP-MS, was around 4 mg $g_{catalyst}{}^{-1}$ for both samples. The textural properties including surface area, pore volume, and pore size were investigated by N_2-physisorption. Figure 3 displays the result for Pd-chitin-500. A type IV isotherm and type II adsorption hysteresis were representative of the formation of a mesoporous material. The same held true for Pd-chitin-Na_2CO_3-500. Both samples exhibited a remarkably high surface area of 452–498 m^2g^{-1}, while the range of pore diameter (4.9–5.3 nm) further proved the occurrence of mesoporous solids.

Table 1. Textural properties, particle size, and palladium content of the catalytic materials.

Material	S_{BET} [m^2g^{-1}] [a]	D_{BJH} (nm) [b]	V_{BJH} [cm^3/g] [c]	*Pd conc.*/mg g^{-1} [d]	*Pd Particle Size* (nm) [e]
Pd-chitin-500	498	4.9	0.61	4.3	9.7
Pd-chitin-Na_2CO_3-500	452	5.3	0.53	3.9	6.7

[a] S_{BET}: specific surface area was calculated using the Brunauer-Emmett-Teller (BET) equation. [b] D_{BJH}: mean pore size diameter was calculated using the Barret-Joyner-Halenda (BJH) equation. [c] V_{BJH}: pore volumes were calculated using the Barret-Joyner-Halenda (BJH) equation. Pd concentrations were determined by [d] ICP-OES and [e] Pd particle size was calculated using XRD analyses employing the Scherrer Equation.

The smaller size of palladium particles in Pd-chitin-Na_2CO_3-500 was correlated to an occlusion phenomenon in the carbonaceous matrix, which plausibly led to a higher mean pore diameter and a slightly lower surface area, in comparison with the Pd-chitin analogue.

Overall, the characterization studies confirmed the suitability of the mechanochemically assisted protocol for the preparation of supported metal nanoparticles on a mesoporous N-doped carbon-base matrix [50,51].

A well-known C-C bond-forming reaction, such as Suzuki-Miyaura cross-coupling, was selected as a model to test the activity of the Pd-based materials. The same approach used for the synthesis of the catalysts, i.e., mechanochemistry based on extrusion, was considered to carry out the reactions. Figure 4 summarizes the design of the experiments. A mixture of phenyl boronic acid (366 mg, 3 mmol), iodobenzene (408 mg, 2 mmol), and the Pd-based catalyst (40 mg) was fed to a mini-extruder heated to 80 °C, the conveying screws

of which were set to 50 rpm at a torque of 2 Nm. The residence time was 1 h. Other tests were performed by adding K_2CO_3 (53 mg, 0.5 mmol). The use of an extra base reactant is reported by most, if not all, protocols for the Suzuki-Miyaura process. The extrudate was collected in the form of a solid. A portion of this material (100 mg) was rinsed with ethanol as a solvent (5 mL). The resulting solution was analyzed by GC-FID and GC-MS to evaluate the conversion and the selectivity, and to assign the structure of the products. The most representative results are reported in Table 2.

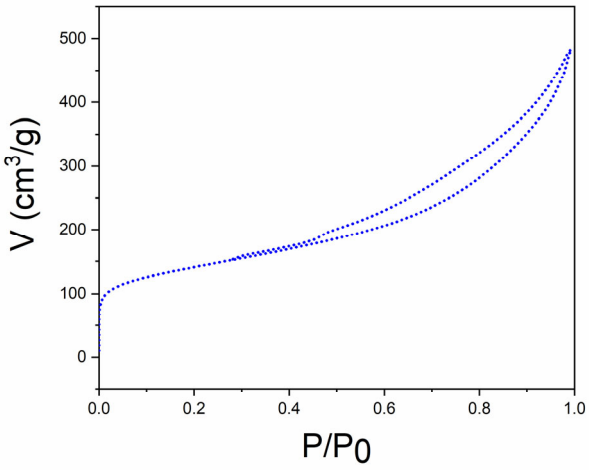

Figure 3. N_2 physisorption isotherm of Pd-chitin-500 sample.

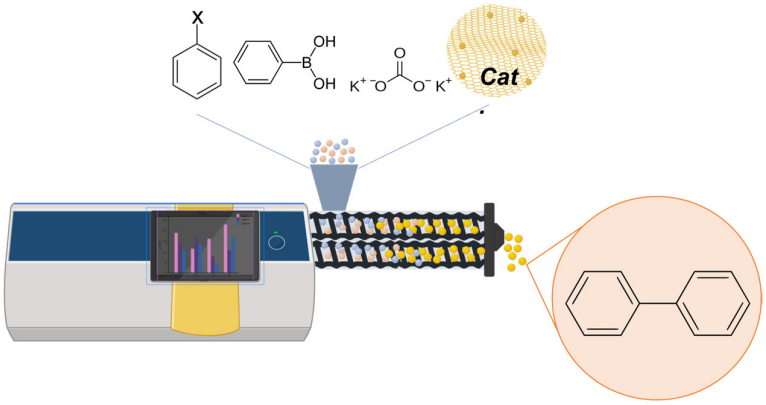

Figure 4. The design of the mechanochemically assisted catalytic Suzuki-Miyaura cross-coupling reaction.

Table 2. The Suzuki-Miyaura cross-coupling under mechanochemistry conditions based on extrusion.

Entry	Catalyst	Base	Conversion (%) [a]	Selectivity (%) [b]
1	Pd-chitin-500	/	<10	>99
2	Pd-chitin-Na_2CO_3	/	<10	>99
3	Pd-chitin-Na_2CO_3-500	/	<10	>99
4	Pd-chitin	K_2CO_3	73	>99
5	**Pd-chitin-500**	**K_2CO_3**	**81**	**>99**
6	Pd-chitin-Na_2CO_3-500	K_2CO_3	78	>99

Reaction conditions: Iodobenzene (2 mmol); $PhB(OH)_2$ (3 mmol); K_2CO_3 (4 mmol); Catalysts amount: 40 mg, 80 °C, 50 rpm, residence time 1 h. [a,b] Conversion of iodobenzene and selectivity to biphenyl were determined by GC. The best catalytic result is highlighted in bold.

All reactions provided the expected product, biphenyl, with >99% selectivity (setails on the characterization of the product are in the SI section), though the conversion was largely affected by the experimental conditions. The reaction outcome was not satisfactory without an added base (entries 1–3); regardless of the use of calcined or not calcined catalysts and the presence/absence of Na_2CO_3 incorporated in the samples, the cross-coupling proceeded to a very limited extent, with a conversion not exceeding 10%. The catalyst preparation was modified using K_2CO_3 in place of Na_2CO_3. This change, however, did not impact on the reaction outcome; the activity of the newly prepared sample was as low as that of Pd-chitin-Na_2CO_3-500. In the presence of K_2CO_3 as an extra base, however, the conversion of iodobenzene was remarkably improved to 73 and 81% using Pd-chitin and Pd-chitin-500, respectively, with an overall biphenyl productivity of up to 41 mmol g_{cat}^{-1} h^{-1} (entries 4 and 5). This clearly confirmed the role of excess (free) base for the cross-coupling process. According to the most accepted mechanistic hypothesis, the base assists the activation of boronic acid, enabling a Pd-B transmetallation step which is critical for the C-C bond formation. Although there are still uncertainties about the occurrence of such a step, a plausible pathway has been proposed whereby the reaction of the base with the organoboron compound produces an anionic organoboronate species which, in turn, performs a nucleophilic attack on a Pd-halide intermediate [52,53].

Overall, our findings not only proved the suitability of the extrusion-assisted protocol to perform the reaction, but it demonstrated that: (i) the base fundamental for the reaction was effective only when added as such and could in no way be made available by incorporating it in the solid catalyst; (ii) the basic sites on the N-doped carbon used as a support were moderately, if at all, involved in the investigated cross-coupling process; and (iii) the calcined catalysts performed slightly better than non-calcined ones. This was highlighted once the reaction took place at a substantial conversion ($\geq$70%) and was even corroborated by the behavior of Pd-chitin-Na_2CO_3-500 (calcined) sample, of which a 78% conversion was reached (entry 6), thereby suggesting that the thermal activation used to prepare the former (calcined) samples made the metal nanoparticles dispersed on them more accessible and active for catalysis. An additional test was carried out by employing $Pd(OAc)_2$ (4 mg) as a catalyst in place of Pd-chitin-500, though the iodobenzene:Pd molar ratio was kept unaltered. Other conditions can be seen in Table 2 (80 °C, 50 rpm, residence time 1 h). The reaction proceeded with both quantitative conversion and selectivity, thereby indicating (as expected) that the availability of the active sites on the acetate complex was superior to that of the heterogenous system. The use of $Pd(OAc)_2$, however, suffered from the well-known disadvantages associated to homogeneous catalysts including the very difficult separation from the product and the virtually impossible reuse for subsequent reactions. For comparison, this last aspect (catalyst recycle) was explored with the heterogenous Pd-chitin-500 system. Under the conditions of entry 5 in Table 2, once the reaction was complete, the catalyst was washed, dried, and reused without any further treatment, and a second reaction was run in exactly the same way as the first one (entry 5). The recycle test confirmed that Pd-chitin-500 preserved its original activity yielding an iodobenzene conversion and a biphenyl selectivity of 79% and >99%, respectively. Moreover, the stability of the used catalyst was examined by comparing its Pd content to that of the fresh catalyst: ICP-OES analyses proved that a negligible metal leaching (<5%) occurred (4.1 and 4.3 mg_{Pd} g^{-1}, for the used and the fresh catalyst, respectively).

Pd-chitin-500 was also tested using bromobenzene and chlorobenzene in place of iodobenzene as a reactant. Under the conditions of entry 5, however, the reactions showed a negligible conversion (ca. 5%) consistent with the general effect of the halide as a leaving group in the Suzuki-Miyaura cross-coupling reactions [52]. Thereafter, to gather further information on the general applicability of the protocol, the organoborane reaction partner was changed. An additional experiment was run by coupling iodobenzene with *m*-tolylboronic acid in place of phenylboronic acid. The test was successful; the conversion was 75% and the selectivity towards the desired product, 3-methyl-1,1′-biphenyl, was 95% (details on the characterization of the product are in the SI section). This proved

that, under the reactive extrusion conditions, the onset of secondary reactions, such as the homocoupling of aryl boronic acids, was not significant.

An additional experiment was designed to test the activity of Pd-chitin-500 also under conventional batch conditions. Accordingly, the same reactants mixture used in Table 2 [phenyl boronic acid (43 mg, 0.35 mmol), iodobenzene (51 mg, 0.25 mmol), K_2CO_3 (70 mg, 0.50 mmol), and the catalyst (10 mg)] was set to react in a 10 mL glass flask, at 80 °C for 1 h, using ethanol (3 mL) as the solvent. The reaction proceeded with complete selectivity to biphenyl, but the reaction conversion was only 58%, ca. 25% lower than that achieved under the reactive extrusion conditions of entry 5 in Table 2. This result, plausibly due to a solvation/dilution effect, highlighted the higher efficiency of the mechanochemical approach compared to traditional procedures in a solution.

4. Conclusions

Mechanochemistry is among the strategies working towards the innovative design of sustainable and cost-efficient synthetic processes. This contribution provides a proof of concept aimed at expanding the applications in this field, using the reactive extrusion that combines the potential of mechanochemistry with the benefits of continuous-flow processes. Albeit at an early stage, the research communication proposed here offers the reliability and reproducibility that demonstrate the suitability of extrusion methods for both the preparation of nanostructured catalysts and the implementation of remarkable catalytic processes for the C-C bond-forming reactions. Supported Pd-based nanoparticles with excellent textural properties (surface area up to 498 $m^2\ g^{-1}$) were prepared via mechanochemistry, in the absence of solvents. Such materials have proven active for the Suzuki-Miyaura cross-coupling of aryl boronic acid with iodobenzene, achieving conversion and selectivity values of up to 81% and 99%, respectively, and a productivity on the desired coupling products of up to 41 mmol $g^{-1}\ h^{-1}$, making them amenable for further scaled up studies of the process.

Supplementary Materials: The following supporting information can be downloaded at: https://www.mdpi.com/article/10.3390/chemistry5030120/s1, Materials and methods, Figure S1: XRD diffractogram of commercial chitin, Figure S2: ^{1}H NMR of biphenyl, Figure S3: ^{13}C NMR of biphenyl, Figure S4: MS spectra (EI, 70 eV) of 3-Methyl-1,1′-biphenyl, Video S1: Mechanochemical synthesis of the catalytic material.

Author Contributions: Conceptualization, D.P., D.R.-P. and M.S.; methodology, D.P.; software, E.R.-C.; validation, A.P., M.S. and E.R.-C.; formal analysis, O.T.; investigation, D.P. and D.R.-P.; resources, A.P., M.S. and E.R.-C.; data curation, D.R.-P.; writing—original draft preparation, D.P. and D.R.-P.; writing—review and editing, D.R.-P. and M.S.; visualization, A.P.; supervision, M.S. and E.R.-C.; project administration, A.P.; funding acquisition, M.S., A.P., E.R.-C. and D.R.-P. All authors have read and agreed to the published version of the manuscript.

Funding: This research was supported by the project H2020-MSCA-COFUND-2019 "Global at Venice- Research and Training for Global Challenges" and by the CUBWAM project funded by Fondazione Cariplo.

Data Availability Statement: Not applicable.

Acknowledgments: D.R.P. acknowledges the project H2020-MSCA-COFUND-2019 "Global at Venice-Research and Training for Global Challenges". We thank the Knowledge Foundation for their financial support.

Conflicts of Interest: The authors declare no conflict of interest.

References

1. Muñoz-Batista, M.J.; Rodriguez-Padron, D.; Puente-Santiago, A.R.; Luque, R. Mechanochemistry: Toward Sustainable Design of Advanced Nanomaterials for Electrochemical Energy Storage and Catalytic Applications. *ACS Sustain. Chem. Eng.* **2018**, *6*, 9530–9544. [CrossRef]
2. Rodríguez-Padrón, D.; Puente-Santiago, A.R.; Caballero, A.; Balu, A.M.; Romero, A.A.; Luque, R. Highly Efficient Direct Oxygen Electro-Reduction by Partially Unfolded Laccases Immobilized on Waste-Derived Magnetically Separable Nanoparticles. *Nanoscale* **2018**, *10*, 3961–3968. [CrossRef] [PubMed]
3. García-Espejo, G.; Rodríguez-Padrón, D.; Luque, R.; Camacho, L.; De Miguel, G. Mechanochemical Synthesis of Three Double Perovskites: $Cs_2AgBiBr_6$, $(CH_3NH_3)_2TlBiBr_6$ and $Cs_2AgSbBr_6$. *Nanoscale* **2019**, *11*, 16650–16657. [CrossRef] [PubMed]
4. Rodríguez-Padrón, D.; Jodlowski, A.D.; De Miguel, G.; Puente-Santiago, A.R.; Balu, A.M.; Luque, R. Synthesis of Carbon-Based Fluorescent Polymers Driven by Catalytically Active Magnetic Bioconjugates. *Green Chem.* **2018**, *20*, 225–229. [CrossRef]
5. Rodríguez-Padrón, D.; Puente-Santiago, A.R.; Balu, A.M.; Romero, A.A.; Muñoz-Batista, M.J.; Luque, R. Benign-by-Design Orange Peellated Nanocatalysts for Continuous Flow Conversion of Levulinic Acid to N-Heterocycles. *ACS Sustain. Chem. Eng.* **2018**, *6*, 16637–16644. [CrossRef]
6. Rodriguez-Padrón, D.; Puente-Santiago, A.R.; Balu, A.M.; Romero, A.A.; Luque, R. Solventless Mechanochemical Preparation of Novel Magnetic Bioconjugates. *Chem. Commun.* **2017**, *53*, 7635–7637. [CrossRef]
7. Caudillo-Flores, U.; Rodríguez-Padrón, D.; Muñoz-Batista, M.J.; Kubacka, A.; Luque, R.; Fernández-García, M. Facile Synthesis of B/g-C_3N_4composite Materials for the Continuous-Flow Selective Photo-Production of Acetone. *Green Chem.* **2020**, *22*, 4975–4984. [CrossRef]
8. Rodríguez-Padrón, D.; Puente-Santiago, A.R.; Caballero, A.; Benítez, A.; Balu, A.M.; Romero, A.A.; Luque, R. Mechanochemical Design of Hemoglobin-Functionalised Magnetic Nanomaterials for Energy Storage Devices. *J. Mater. Chem. A* **2017**, *5*, 16404–16411. [CrossRef]
9. García-Espejo, G.; Rodríguez-Padrón, D.; Pérez-Morales, M.; Luque, R.; De Miguel, G.; Camacho, L. Mechanochemical Synthesis of One-Dimensional (1D) Hybrid Perovskites Incorporating Polycyclic Aromatic Spacers: Highly Fluorescent Cation-Based Materials. *J. Mater. Chem. C* **2018**, *6*, 7677–7682. [CrossRef]
10. Liu, X.; Li, Y.; Zeng, L.; Li, X.; Chen, N.; Bai, S.; He, H.; Wang, Q.; Zhang, C. A Review on Mechanochemistry: Approaching Advanced Energy Materials with Greener Force. *Adv. Mater.* **2022**, *34*, 2108327. [CrossRef]
11. Jiao, Y.; Nan, Y.; Wu, Z.; Wang, X.; Zhang, J.; Zhang, B.; Huang, S.; Shi, J. Mechanochemical Synthesis of Enzyme@covalent Organic Network Nanobiohybrids. *Appl. Mater. Today* **2022**, *26*, 101381. [CrossRef]
12. Espro, C.; Rodríguez-Padrón, D. Re-Thinking Organic Synthesis: Mechanochemistry as a Greener Approach. *Curr. Opin. Green Sustain. Chem.* **2021**, *30*, 100478. [CrossRef]
13. Martín-Perales, A.I.; Balu, A.M.; Malpartida, I.; Luque, R. Prospects for the Combination of Mechanochemistry and Flow Applied to Catalytic Transformations. *Curr. Opin. Green Sustain. Chem.* **2022**, *38*, 100714. [CrossRef]
14. Wang, G.W. Mechanochemical Organic Synthesis. *Chem. Soc. Rev.* **2013**, *42*, 7668–7700. [CrossRef]
15. Andersen, J.; Mack, J. Mechanochemistry and Organic Synthesis: From Mystical to Practical. *Green Chem.* **2018**, *20*, 1435–1443. [CrossRef]
16. James, S.L.; Frišcic, T. Mechanochemistry. *Chem. Soc. Rev.* **2013**, *42*, 7494–7496. [CrossRef]
17. Friščić, T.; Mottillo, C.; Titi, H.M. Mechanochemistry for Synthesis. *Angew. Chem.* **2020**, *132*, 1030–1041. [CrossRef]
18. Do, J.; Titi, H.M.; Auvray, T.; Lennox, C.B.; Cuccia, L.A. Rapid, room-temperature, solvent-free mechanochemical oxidation of elemental gold into organosoluble gold salts †. *Green Chem.* **2023**, *25*, 5774. [CrossRef]
19. Brekalo, I.; Martinez, V.; Karadeniz, B.; Orešković, P.; Drapanauskaite, D.; Vriesema, H.; Stenekes, R.; Etter, M.; Dejanović, I.; Baltrusaitis, J.; et al. Scale-Up of Agrochemical Urea-Gypsum Cocrystal Synthesis Using Thermally Controlled Mechanochemistry. *ACS Sustain. Chem. Eng.* **2022**, *10*, 6743–6754. [CrossRef]
20. Bolt, R.R.A.; Raby-Buck, S.E.; Ingram, K.; Leitch, J.A.; Browne, D.L. Temperature-Controlled Mechanochemistry for the Nickel-Catalyzed Suzuki-Miyaura-Type Coupling of Aryl Sulfamates via Ball Milling and Twin-Screw Extrusion. *Angew. Chem. Int. Ed.* **2022**, *61*, e202210508. [CrossRef]
21. Andersen, J.; Brunemann, J.; Mack, J. Exploring Stable, Sub-Ambient Temperatures in Mechanochemistry: Via a Diverse Set of Enantioselective Reactions. *React. Chem. Eng.* **2019**, *4*, 1229–1236. [CrossRef]
22. Bolt, R.R.A.; Leitch, J.A.; Jones, A.C.; Nicholson, W.I.; Browne, D.L. Continuous Flow Mechanochemistry: Reactive Extrusion as an Enabling Technology in Organic Synthesis. *Chem. Soc. Rev.* **2022**, *51*, 4243–4260. [CrossRef] [PubMed]
23. Vidakis, N.; Petousis, M.; Mountakis, N.; Grammatikos, S.; Papadakis, V.; Kechagias, J.D.; Das, S.C. On the Thermal and Mechanical Performance of Polycarbonate/Titanium Nitride Nanocomposites in Material Extrusion Additive Manufacturing. *Compos. Part C Open Access* **2022**, *8*, 100291. [CrossRef]
24. Galant, O.; Cerfeda, G.; McCalmont, A.S.; James, S.L.; Porcheddu, A.; Delogu, F.; Crawford, D.E.; Colacino, E.; Spatari, S. Mechanochemistry Can Reduce Life Cycle Environmental Impacts of Manufacturing Active Pharmaceutical Ingredients. *ACS Sustain. Chem. Eng.* **2022**, *10*, 1430–1439. [CrossRef]
25. Xu, J.; Hou, S.; Niu, Q.; Zhang, P.; Luo, Z.H. Cyclic Extrusion Synthesis of Mesoporous Carbon-Supported Metal Catalysts for Selective Hydrogenation. *AIChE J.* **2023**, *69*, e18073. [CrossRef]

26. Sonei, S.; Taghavi, F.; Khojastehnezhad, A.; Gholizadeh, M. Copper-Functionalized Silica-Coated Magnetic Nanoparticles for an Efficient Suzuki Cross-Coupling Reaction. *ChemistrySelect* **2021**, *6*, 359–368. [CrossRef]
27. Musza, K.; Szabados, M.; Ádám, A.A.; Kónya, Z.; Kukovecz, Á.; Sipos, P.; Pálinkó, I. Mechanochemically Modified Hydrazine Reduction Method for the Synthesis of Nickel Nanoparticles and Their Catalytic Activities in the Suzuki-Miyaura Cross-Coupling Reaction. *React. Kinet. Mech. Catal.* **2019**, *126*, 857–868. [CrossRef]
28. Beromi, M.M.; Nova, A.; Balcells, D.; Brasacchio, A.M.; Brudvig, G.W.; Guard, L.M.; Hazari, N.; Vinyard, D.J. Mechanistic Study of an Improved Ni Precatalyst for Suzuki-Miyaura Reactions of Aryl Sulfamates: Understanding the Role of Ni(I) Species. *J. Am. Chem. Soc.* **2017**, *139*, 922–936. [CrossRef]
29. Hergert, T.; Varga, B.; Thurner, A.; Faigl, F.; Mátravölgyi, B. Copper-Facilitated Suzuki-Miyaura Coupling for the Preparation of 1,3-Dioxolane-Protected 5-Arylthiophene-2-Carboxaldehydes. *Tetrahedron* **2018**, *74*, 2002–2008. [CrossRef]
30. Liu, F.; Liu, X.; Chen, F.; Fu, Q. Tannic Acid: A Green and Efficient Stabilizer of Au, Ag, Cu and Pd Nanoparticles for the 4-Nitrophenol Reduction, Suzuki-Miyaura Coupling Reactions and Click Reactions in Aqueous Solution. *J. Colloid Interface Sci.* **2021**, *604*, 281–291. [CrossRef]
31. Seo, T.; Ishiyama, T.; Kubota, K.; Ito, H. Solid-State Suzuki-Miyaura Cross-Coupling Reactions: Olefin-Accelerated C-C Coupling Using Mechanochemistry. *Chem. Sci.* **2019**, *10*, 8202–8210. [CrossRef]
32. Seo, T.; Kubota, K.; Ito, H. Mechanochemistry-Directed Ligand Design: Development of a High-Performance Phosphine Ligand for Palladium-Catalyzed Mechanochemical Organoboron Cross-Coupling. *J. Am. Chem. Soc.* **2023**, *145*, 6823–6837. [CrossRef]
33. Zhang, J.; Zhang, P.; Ma, Y.; Szostak, M. Mechanochemical Synthesis of Ketones via Chemoselective Suzuki-Miyaura Cross-Coupling of Acyl Chlorides. *Org. Lett.* **2022**, *24*, 2338–2343. [CrossRef]
34. Zhang, J.; Zhang, P.; Shao, L.; Wang, R.; Ma, Y.; Szostak, M. Mechanochemical Solvent-Free Suzuki-Miyaura Cross-Coupling of Amides via Highly Chemoselective N−C Cleavage. *Angew. Chem. Int. Ed.* **2022**, *61*, e202114146. [CrossRef]
35. Zuliani, A.; Balu, A.M.; Luque, R. Efficient and Environmentally Friendly Microwave-Assisted Synthesis of Catalytically Active Magnetic Metallic Ni Nanoparticles. *ACS Sustain. Chem. Eng.* **2017**, *5*, 11584–11587. [CrossRef]
36. Maschmeyer, T.; Luque, R.; Selva, M. Upgrading of Marine (Fish and Crustaceans) Biowaste for High Added-Value Molecules and Bio(Nano)-Materials. *Chem. Soc. Rev.* **2020**, *49*, 4527–4563. [CrossRef]
37. Polidoro, D.; Perosa, A.; Rodríguez-Castellón, E.; Canton, P.; Castoldi, L.; Rodríguez-Padrón, D.; Selva, M. Metal-Free N-Doped Carbons for Solvent-Less CO2Fixation Reactions: A Shrimp Shell Valorization Opportunity. *ACS Sustain. Chem. Eng.* **2022**, *10*, 13835–13848. [CrossRef]
38. Xu, C.; Nasrollahzadeh, M.; Selva, M.; Issaabadi, Z.; Luque, R. Waste-to-Wealth: Biowaste Valorization into Valuable Bio(Nano)Materials. *Chem. Soc. Rev.* **2019**, *48*, 4791–4822. [CrossRef]
39. Rodríguez-Padrón, D.; Zhao, D.; Carrillo-Carrion, C.; Morales-Torres, C.; Elsharif, A.M.; Balu, A.M.; Luque, R.; Len, C. Exploring the Potential of Biomass-Templated Nb/ZnO Nanocatalysts for the Sustainable Synthesis of N-Heterocycles. *Catal. Today* **2021**, *368*, 243–249. [CrossRef]
40. Martín-Perales, A.I.; Rodríguez-Padrón, D.; García Coleto, A.; Len, C.; De Miguel, G.; Muñoz-Batista, M.J.; Luque, R. Photocatalytic Production of Vanillin over CeOxand ZrO_2Modified Biomass-Templated Titania. *Ind. Eng. Chem. Res.* **2020**, *59*, 17085–17093. [CrossRef]
41. Cárdenas, G.; Cabrera, G.; Taboada, E.; Miranda, S.P. Chitin Characterization by SEM, FTIR, XRD, And13C Cross Polarization/Mass Angle Spinning NMR. *J. Appl. Polym. Sci.* **2004**, *93*, 1876–1885. [CrossRef]
42. Cui, D.; Yang, J.; Lu, B.; Deng, L.; Shen, H. Extraction and Characterization of Chitin from Oratosquilla Oratoria Shell Waste and Its Application in *Brassica campestris* L.ssp. *Int. J. Biol. Macromol.* **2022**, *198*, 204–213. [CrossRef] [PubMed]
43. Tamoradi, T.; Ghorbani-Choghamarani, A.; Ghadermazi, M. Synthesis of a New Pd(0)-Complex Supported on Magnetic Nanoparticles and Study of Its Catalytic Activity for Suzuki and Stille Reactions and Synthesis of 2,3-Dihydroquinazolin-4(1H)-One Derivatives. *Polyhedron* **2018**, *145*, 120–130. [CrossRef]
44. Baruah, D.; Das, R.N.; Hazarika, S.; Konwar, D. Biogenic Synthesis of Cellulose Supported Pd(0) Nanoparticles Using Hearth Wood Extract of Artocarpus Lakoocha Roxb—A Green, Efficient and Versatile Catalyst for Suzuki and Heck Coupling in Water under Microwave Heating. *Catal. Commun.* **2015**, *72*, 73–80. [CrossRef]
45. Polidoro, D.; Rodriguez-Padron, D.; Perosa, A.; Luque, R.; Selva, M. Chitin-Derived Nanocatalysts for Reductive Amination Reactions. *Materials* **2023**, *16*, 575. [CrossRef]
46. Masood, M.H.; Haleem, N.; Shakeel, I.; Jamal, Y. Carbon Dioxide Conversion into the Reaction Intermediate Sodium Formate for the Synthesis of Formic Acid. *Res. Chem. Intermed.* **2020**, *46*, 5165–5180. [CrossRef]
47. Kirik, S.D.; Mulagaleev, R.F.; Blokhin, A.L. $[Pd(CH_3COO)_2]_n$ from X-Ray Powder Diffraction Data. *Acta Crystallogr. Sect. C Cryst. Struct. Commun.* **2004**, *60*, 449–450. [CrossRef]
48. Kibasomba, P.M.; Dhlamini, S.; Maaza, M.; Liu, C.P.; Rashad, M.M.; Rayan, D.A.; Mwakikunga, B.W. Strain and Grain Size of TiO_2 Nanoparticles from TEM, Raman Spectroscopy and XRD: The Revisiting of the Williamson-Hall Plot Method. *Results Phys.* **2018**, *9*, 628–635. [CrossRef]
49. Holzwarth, U.; Gibson, N. The Scherrer Equation versus the "Debye-Scherrer Equation." *Nat. Nanotechnol.* **2011**, *6*, 534. [CrossRef]
50. Karandikar, P.; Patil, K.R.; Mitra, A.; Kakade, B.; Chandwadkar, A.J. Synthesis and Characterization of Mesoporous Carbon through Inexpensive Mesoporous Silica as Template. *Microporous Mesoporous Mater.* **2007**, *98*, 189–199. [CrossRef]

51. Polidoro, D.; Ballesteros-Plata, D.; Perosa, A.; Rodríguez-Castellón, E.; Rodríguez-Padrón, D.; Selva, M. Controlled Alcohol Oxidation Reactions by Supported Non-Noble Metal Nanoparticles on Chitin-Derived N-doped Carbons. *Catal. Sci. Technol.* **2023**, *13*, 2223–2238. [CrossRef]
52. Bao, G.; Bai, J.; Li, C. Synergistic Effect of the Pd-Ni Bimetal/Carbon Nanofiber Composite Catalyst in Suzuki Coupling Reaction. *Org. Chem. Front.* **2019**, *6*, 352–361. [CrossRef]
53. D'Alterio, M.C.; Casals-Cruañas, È.; Tzouras, N.V.; Talarico, G.; Nolan, S.P.; Poater, A. Mechanistic Aspects of the Palladium-Catalyzed Suzuki-Miyaura Cross-Coupling Reaction. *Chem. A Eur. J.* **2021**, *27*, 13481–13493. [CrossRef]